Langevin Dynamics Simulations of the Diffusion of Molecular Knots in Tensioned Polymer Chains†

Lei Huang and Dmitrii E. Makarov*

Department of Chemistry and Biochemistry and Institute for Theoretical Chemistry, University of Texas at Austin, Austin, Texas 78712

Received: March 9, 2007; In Final Form: June 4, 2007

Motivated by recent experiments, in which knots have been tied in individual biopolymer molecules, we use Langevin dynamics simulations to study the diffusion of a knot along a tensioned polymer chain. We find that the dependence of the knot diffusion coefficient on the tension can be non-monotonic. This behavior can be explained by the model, in which the motion of the knot involves cooperative displacement of a local knot region. At low tension, the overall viscous drag force that acts on the knot region is proportional to the number N of monomers that participate in the knot, which decreases as the tension is increased, leading to faster diffusion. At high tension the knot becomes tight and its dynamics are dominated by the chain's internal friction, which increases with the increasing tension, thereby slowing down the knot diffusion. This model is further supported by the observation that the knot diffusion coefficient measured across a set of different knot types is inversely proportional to N. We propose that the lack of tension dependence of the knot diffusion coefficients measured in recent experiments is due to the fact that the experimental values of the tension are close to the turnover between the high- and low-force regimes.

1. Introduction

Molecular knots tied in individual polymer strands have attracted the attention of many physicists, chemists, and molecular biologists.[1−15] The importance of knots as topological defects that affect polymers' dynamics has been recognized in a number of contexts. They may, for example, impede DNA replication (see, for example, ref 2 and references therein) or lead to long-time memory effects in polymer melts.[9,16] From a polymer theory perspective, a number of fascinating issues exist that deal with the scaling properties of random knots (see, for example, refs 2, 11, 13). Recently, molecular knots have been created and observed at a single molecule level.[17,18] In particular, knots tied in DNA chains with optical tweezers were seen to undergo diffusive motion, and the diffusion coefficients have been measured for different types of knots.[18] Those experiments have motivated several theoretical and simulation studies of knot dynamics in polymers.[8,12,19] Vologodskii[8] has used Brownian dynamics simulations to study knot diffusion in DNA and found the computed diffusion coefficients for different types of knots to agree with the experimental values to within a factor of 2. Metzler et al.[12] have presented general theoretical considerations of different mechanisms that may affect knot mobility. The aim of the present work is to undertake a more systematic study of the effects of the knot type, the tension in the chain, and the polymer's flexibility on the knot diffusion.

Consider a knot tied in a polymer chain, whose persistence length l_p is longer than the distance between two neighboring monomers σ and whose contour length is much longer than l_p. Suppose the two chain ends are pulled apart with a force f. As the value of this force is increased, three physical regimes are encountered:

1. The "blob" regime,[12] $f \ll k_BT/l_p$. In this regime the force is too low to straighten the chain so that locally, within a blob of size[20] $\sim k_BT/f$, the chain behaves as a random coil that is unaffected by the force. If a knot is tied in such a chain, it will be likely to collide with other segments of the chain and its size will fluctuate significantly. The $f = 0$ case has been addressed in refs 16, 21 showing that knot loosening and large size fluctuations can be important in the unknotting mechanism.

2. The "elastic regime". In this regime, the force becomes high enough, $f > k_BT/l_p$, to align the segments of the chain in the general direction of the force. Thermal fluctuations are unlikely to cause collisions of different chain segments except for the monomers constrained within the knot. In this regime, the knot size is determined by the bending elasticity of the chain vs the force. Imagine a knot tied in a guitar string. The harder one pulls at the ends of the string, the smaller the knot. The higher the bending stiffness (and, consequently, the persistence length), the larger the knot.

3. The tight knot regime. Finally, when the force becomes very high, the knot size will no longer significantly change as its size will be dominated by the repulsive interactions between the contacting monomers in the knot. This is similar to an "ideal knot" in a flexible rope, where its size is determined by the thickness of the rope (see, e.g., refs 7, 22).

The blob regime is not considered in the rest of this paper. A double-stranded DNA with a persistence length of ∼50 nm will be in the blob regime only at forces $f < k_BT/l_p \sim 0.08$ pN that are lower than the forces used in the experiments described in ref 18.

Between the elastic and the tight knot regimes, we commonly observe a turnover behavior, where the knot diffusion coefficient first increases and then decreases as the applied tension f is increased. This behavior can be understood if one assumes that the knot diffusion is accomplished via concerted motion of a local knot region[12] so that the total friction drag force that acts

† Part of the special issue "Robert E. Wyatt Festschrift".

* Corresponding author. Tel: 512-471-4575. Fax: 512-471-8696. E-mail: makarov@mail.cm.utexas.edu.

10.1021/jp071940+ CCC: $37.00
Published on Web 07/19/2007

on the knot is proportional to the number N of monomers within the knot multiplied by the friction coefficient ξ_0 per single monomer. (A more precise definition of the effective number N of monomers in the knot will be given in subsequent sections). The knot diffusion coefficient is then given by the Einstein formula:

$$D \simeq \frac{k_B T}{N\xi_0} \tag{1}$$

In the elastic regime, increasing the tension reduces the knot length N, thereby accelerating the diffusion. As the tight knot limit is approached, the increased repulsive interactions among the monomers within the knot region result in a "bumpier" energy landscape for the knot translation, which can be interpreted as an increased "internal friction".[23,24] This leads to slower diffusion. Interestingly, we find here that in the tight knot regime the diffusion coefficient depends only on the knot length N rather than separately on the chain persistence length and the tension.

In the following sections we will present our data and describe simple theoretical arguments to rationalize our findings. We will further show that our results can shed light on some of the experimental observations made in ref 18, such as the dependence of the diffusion coefficient on the knot type and the apparent lack of its tension dependence.

The rest of this paper is organized as follows. Section 2 describes how the simulations were performed. Our results are presented in Section 3. Section 4 concludes with a comparison of our results with experiments.

2. Methods

The Model. Our model of a polymer chain consists of $L = 90$ beads and is described by the potential

$$V(\mathbf{r}_1,\mathbf{r}_2,..,\mathbf{r}_L) = V_{\text{bond}} + V_{\text{bend}} + V_{\text{nonbonded}} \tag{2}$$

as a function of the positions $\mathbf{r}_i$ of each bead. The first term

$$V_{\text{bond}} = \sum_{i=2}^{L} \left(k_b(|\mathbf{r}_i - \mathbf{r}_{i-1}| - \sigma)^2/2 + k_h\left(\frac{|\mathbf{r}_i - \mathbf{r}_{i-1}| - \sigma}{\Delta b}\right)^6 \right) \tag{3}$$

is an anharmonic potential that describes bond stretching. Here, σ is the equilibrium bond length, $\Delta b = 0.25\sigma$, $k_b = 100\epsilon/\sigma^2$, $k_h = 2\epsilon$, and ϵ is a parameter that sets the energy scale. We use the bending potential

$$V_{\text{bend}} = k \sum_{i=2}^{L-1} k_\theta(\theta_i - \theta^0)^2/2 \tag{4}$$

to vary the polymer's persistence length by adjusting the value of the dimensionless bending stiffness k. Here, $k_\theta = 4.8\epsilon/\text{rad}^2$ and θ_i is the angle between the bond vectors $\mathbf{r}_i - \mathbf{r}_{i-1}$ and $-(\mathbf{r}_{i+1} - \mathbf{r}_i)$, whose equilibrium value is $\theta^0 = \pi$. Finally, excluded volume effects are incorporated by using a purely repulsive potential between the beads that are not bonded:

$$V_{\text{nonbonded}} = \sum_{|i-j|\geq 2} 4\epsilon\left(\left(\frac{\sigma}{\left(\left|\mathbf{r}_i - \mathbf{r}_j\right|\right)}\right)^{12} - \left(\frac{\sigma}{\left|\mathbf{r}_i - \mathbf{r}_j\right|}\right)^6 + \frac{1}{4}\right) S\left(\left|\mathbf{r}_i - \mathbf{r}_j\right|\right) \tag{5}$$

where $S(x)$ is a step function defined as

$$S(x) = \begin{cases} 1, x \leq 2^{1/6}\sigma \\ 0, x > 2^{1/6}\sigma \end{cases} \tag{6}$$

The dynamics of the chain were generated by solving the Langevin equation of the form

$$m\ddot{\mathbf{r}}_i(t) = -\xi_0\dot{\mathbf{r}}_i(t) - \frac{\partial(V + V_{\text{stretch}})}{\partial \mathbf{r}_i} + \mathbf{R}(t) \tag{7}$$

where m is the monomer mass, ξ_0 is the friction coefficient for each monomer (whose value is set to $\xi_0 = 2.0(\sigma^2/m\epsilon)^{-1/2}$), $\mathbf{R}(t)$ is a random δ-correlated, Gaussian-distributed force satisfying the fluctuation−dissipation theorem, and $V_{\text{stretch}} = -f(z_L - z_1)$ is a stretching potential that describes a force f that pulls the first and the Lth monomers apart. The z-axis coincides with the direction of the force. In the following, we report all of our results using dimensionless units of energy, distance, time, and force set by ϵ, σ, $\tau = (m\sigma^2/\epsilon)^{1/2}$, and $f_0 = \epsilon/\sigma$, respectively. All of the simulations were performed at the same temperature equal to $T = 1.0\epsilon/k_B$.

The presence of a knot in the chain was monitored by using the program of Harris and Harvey[25] that uses the method of Vologodskii et al.[26] to calculate the Alexander polynomial. Animations of the simulated dynamics of knotted polymers are available as Supporting Information.

The Diffusion Coordinate. To describe the movement of the knot as a one-dimensional diffusion process, we first need to specify the coordinate along which it diffuses. Two obvious choices exist: (i) monitor the projection z of the knot position on the direction of the applied force, or (ii) monitor the knot diffusion along the polymer chain by using a discrete monomer index n as the diffusion coordinate. In the limit of a very high force, the two coordinates are equivalent as the shape of the chain away from the knot region is nearly a straight line. In the blob regime, the two diffusion coordinates would be drastically different. Generally, the diffusion projected onto the axis z will appear to be slower than the diffusion along the chain itself. In the range of forces used here, the difference is about 15% for the lowest force used.

Choice (i) may be closer to the experimental measurements. However, another, more subtle point should be considered. To use definition (i), one has to specify the reference frame with respect to which z is determined. This can be the laboratory frame, the chain's center of mass, or the position of one of the chain ends. The difference between these should disappear in the limit of a very long chain, where the translations of the entire chain can be neglected. However, for practical reasons our chain cannot be too long in a simulation, and for chains of finite length all three definitions give different results. The "internal" diffusion coordinate (ii) is, however, uniquely defined and can be used to determine the time it takes the knot to escape off the chain ends. For this reason, we use the second choice for the diffusion coordinate here while keeping in mind that

some of the results may be affected by the particular way of measuring the diffusion coefficient.

Finally, since knots have finite size, we need to specify how the knot position is described in terms of a single point in space. To do so, we define the boundaries of the knot region, n_l and n_r, as illustrated in Figure 1. The knot coordinate along the chain is then defined as $n = (n_l + n_r)/2$.

Determination of the Knot Diffusion Coefficient. We have used two methods of computing the knot diffusion coefficient. The first method uses the relationship

$$D = \langle [n(\Delta t) - n(0)]^2 \rangle / (2\Delta t) \tag{8}$$

where the square of the knot displacement $n(\Delta t) - n(0)$ is averaged over a series of short-time simulations, with the knot initially located at $n(0)$. Metzler et al.[12] have considered various knot diffusion mechanisms and have predicted that the diffusion should become faster near the chain ends. When the knot is close to a chain end, it can become untied though a cooperative motion of the dangling chain segment. This untying mechanism should become increasingly more likely as the distance from the chain ends becomes smaller than the length of the knot itself.[12] In this regime, however, one cannot view the knot as a point object, and eq 8 cannot be used to determine the value of D. For this reason, the diffusion coefficients reported here have always been calculated in the regime where such boundary effects could be neglected (i.e., when the knot is sufficiently far from the chain ends). In this regime, we find that the knot diffusion coefficient calculated from eq 8 is insensitive to the knot's initial location $n(0)$. Furthermore, we found no significant dependence of the diffusion coefficient on the overall chain length L.

An alternative way of determining D is to consider the probability distribution $p_{esc}(t)$ for the time t it takes for the knot to escape off the ends of the chain, provided that at $t = 0$ the knot was placed in the middle of the chain, $n(0) = L/2$. To avoid the boundary effects mentioned above, instead of considering the entire chain one can specify a chain segment $((L - l)/2,(L + l)/2)$ such that the chain's extremities are excluded from the consideration. We place the knot in the middle of the chain, $n(0) = L/2$, and follow its dynamics until it reaches one of the segment boundaries, $n(t) = (L - l)/2$ or $(L + l)/2$, for the first time. If the motion of the knot can be viewed as free diffusion, then the probability distribution $p_{esc}(t)$ of the time t it takes to reach a boundary can be obtained by solving the free diffusion equation with absorbing boundary conditions (see Appendix A) and the value of D can be obtained from a fit of the simulated $p_{esc}(t)$. If the diffusion coefficient along the chain were not constant or there were a deterministic biasing force driving the knot in the direction of, or away from, the chain center, then we would expect to see the simulated $p_{esc}(t)$ to deviate from the solution of the diffusion equation with a constant D. As shown in Appendix A, we could not find any noticeable deviations from the free diffusion model in the range of forces studied and the value of D determined this way was the same as that estimated from eq 8. Furthermore, we found that the boundary effects due to the chain extremities have no noticeable effect on $p_{esc}(t)$. In other words, the probability for the knot to escape off the chain ends is still described well by the solution of a one-dimensional diffusion equation with a constant D whose value is close to that estimated from eq 8.

A tension in a knotted chain compacts the knot. We expect that the boundary effects predicted in ref 12 would become pronounced at low or zero tension. However, since in this regime the knot size would become comparable with the relatively short chain length used here, the diffusion coefficient in such low-force limit cannot be meaningfully extracted from the simulations reported here.

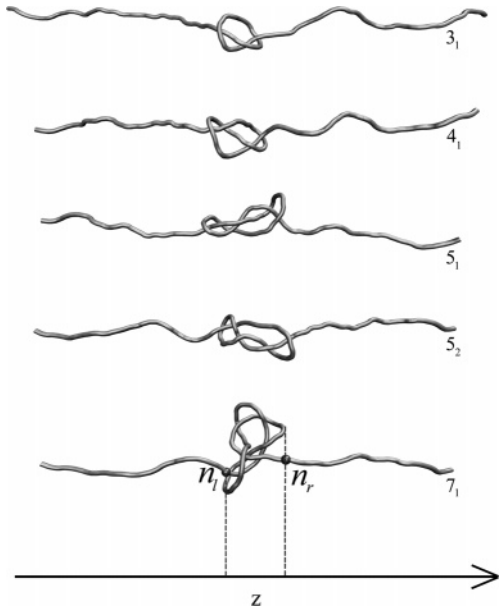

Figure 1. Snapshots of the knots of different types studied here. Definition of the knot boundaries n_l and n_r is also illustrated.

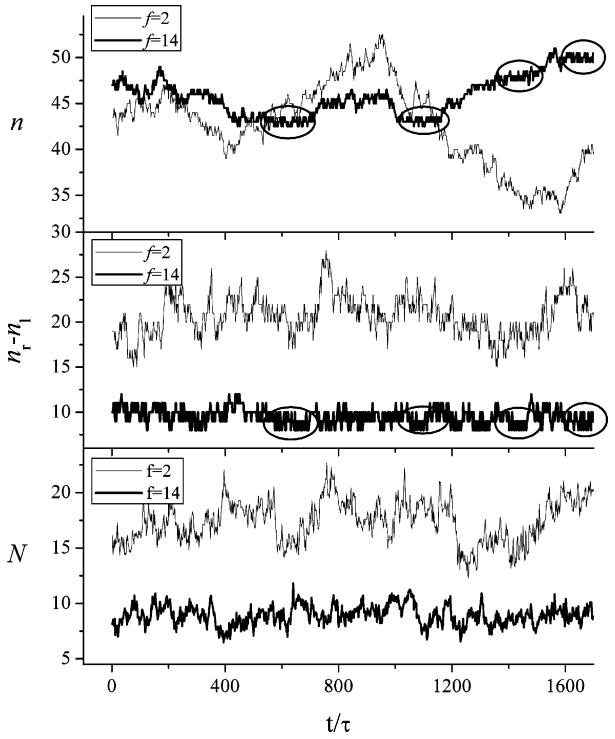

Figure 2. (Top) Typical knot trajectories $n(t)$ at low and high forces ($k = 2$ in each case). Circles indicate the stalling events that are observed in the high-force case. (Middle) Fluctuations in the instantaneous knot length defined as the chain contour length $n_r - n_l$ between the knot boundaries for the same trajectories. (Bottom) Fluctuations in the instantaneous knot length N as defined by eq 9 for the same trajectories.

3. Results

Knot Trajectories. Animations of knot trajectories obtained at two different values of the force are available as Supporting Information. In Figure 2, we show the time dependence of the knot position $n(t)$ for two typical trajectories, one taken at a

low-force value and the other at a high-force value corresponding to the tight knot regime. In the latter case, stalling events are observed, in which the knot becomes trapped in a certain configuration and then escapes it through a thermal fluctuation. Also shown in this figure is the time dependence of the instantaneous knot length for the same trajectories. Two definitions of the knot length are used, one being simply the contour length of the chain between the knot boundaries, $n_r - n_l$, and the other is based on the sliding knot model and is defined below. It is seen that the knot size can fluctuate significantly and that the knot tends to be tighter during the stalling events.

Dependence of the Diffusion Coefficient on the Knot Length. Several knot diffusion mechanisms have been proposed by others,[12,18] involving either cooperative motions of large portions of the entire chain or local motions of a knot region. If the knot translation involves concerted motion of a chain segment that contains N monomers, then the effective friction coefficient for this segment should be $\xi \sim N\xi_0$, where ξ_0 is the friction coefficient per one monomer (defined in eq 7). We then expect the effective knot diffusion coefficient to be approximately given by eq 1. If the local mechanism dominates, then N should be of the order of the knot length, that is, the number of monomers engaged in the knot.

To test the validity of eq 1, we then need a way of measuring the effective knot length N. One possibility is to simply use the contour length of the chain between the knot boundaries, $n_r - n_l$. The problem with this is that our purely geometric definition of the knot boundaries is somewhat arbitrary. While the average knot position $n = (n_l + n_r)/2$ is not significantly affected by the precise choice of the boundaries, this is not necessarily true for the knot length.

A more physically meaningful definition of the knot length that we use here is based on the sliding knot model described in Appendix B. In this model, the knot slides along the chain without changing its shape while the chain ends are not moving. Even in this simple model, different chain segments move with different velocities so N cannot be simply taken to be the number of monomers that move. As shown in Appendix B, the total viscous drag force that acts on the chain when the knot moves with a velocity v is equal to $-\xi_0 N v$, where N is given by

$$N = L\left(1 - \frac{\Delta z_{\text{knotted}}}{\Delta z_{\text{unknotted}}}\right) \tag{9}$$

Here $\Delta z_{\text{knotted}}$ and $\Delta z_{\text{unknotted}}$ is the extension of the chain with and without knot, respectively. In other words, the effective length of the chain segment involved in the knot motion is the difference between the lengths of the unknotted and knotted chains. Coincidentally, this measure of the knot length was used in ref 18 to estimate the knot length from experimental DNA knot images. While eq 9 does not give the correct length of the knotted chain segment,[7,18] it turns out to be the proper knot length measure to be used in eq 1, at least within the sliding knot model. Since, unlike the sliding knot model, the chain fluctuates in our case, the knot length measure that we adopt in practice uses the average chain extensions measured along the direction of the force for $\Delta z_{\text{knotted}}$ and $\Delta z_{\text{unknotted}}$. The instantaneous knot length used in Figure 2 is obtained by using the instantaneous value of $\Delta z_{\text{knotted}}$ instead of its mean.

To vary the knot length N we now change the bending stiffness k (see eq 4) while keeping the applied tension constant. The resulting dependence of the knot diffusion coefficient on k is shown in Figure 3. As k is increased, the chain becomes stiffer

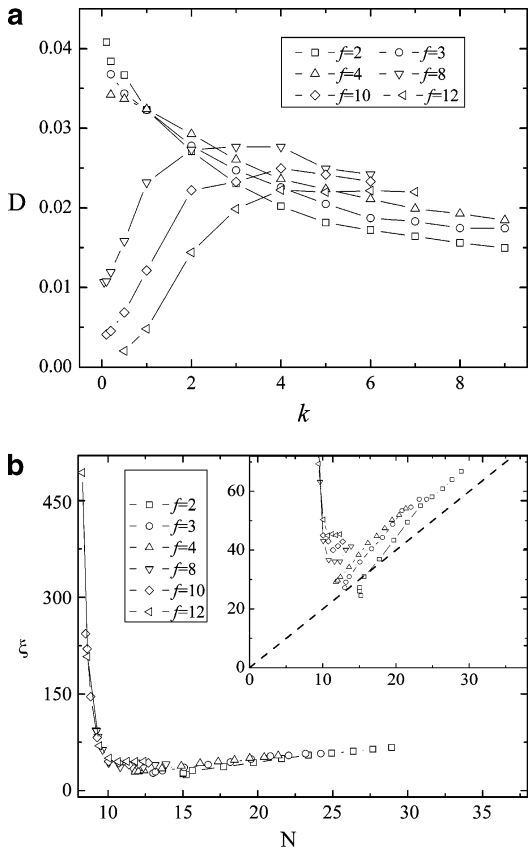

Figure 3. (a) The dependence of the diffusion coefficient of the knot of type 3_1 on the bending spring constant k for different values of the tension f. The units are explained in the Methods section. (b) Same data as in (a) plotted as the effective friction coefficient $\xi = k_B T/D$ vs the knot length N. The dashed line is given by the equation $\xi = \xi_0 N$, where ξ_0 is the friction coefficient per one monomer (cf., eq 7). Inset: Same plot with the ξ scale blown up.

and the knot length N becomes larger. According to eq 1, this should result in a decreasing value of D. Indeed, we observe a monotonically decreasing $D(k)$ when the applied tension f is sufficiently low. For high f, the observed dependence $D(k)$ is non-monotonic, showing a maximum at a certain value of the chain stiffness.

In Figure 3b we plot the effective friction coefficient $\xi = k_B T/D$ as a function of the knot length N for the same data. According to eq 1, we expect ξ to be proportional to N. Indeed, the dependence $\xi(N)$ is close to a straight line $\xi(N) = \xi_0 N$ (shown as a dashed line in the inset of Figure 3b) for knots that are not too tight (i.e., for sufficiently large N). For tight knots (small N) the behavior of $\xi(N)$ is entirely different, showing the opposite trend for more compact knots to diffuse more slowly. This behavior of tight knots will be discussed below.

Dependence of the Diffusion Coefficient on the Tension in the Chain. The tension dependence of the diffusion coefficient is shown in Figure 4a for different values of the bending spring constant k. When the chain is sufficiently stiff (i.e., its persistence length is long), D is a non-monotonic function of the tension. The initial rise of $D(f)$ at low forces is consistent with eq 1 since an increased tension tightens the knot thus reducing its length N. This is further illustrated in Figure 4b, which shows the effective friction coefficient ξ as a function of the knot length N for the same data. For stiff chains and large N (i.e., low force f), we observe that ξ is an increasing function of N, behaving very similarly to the dependence $\xi(N)$ seen in Figure 3b.

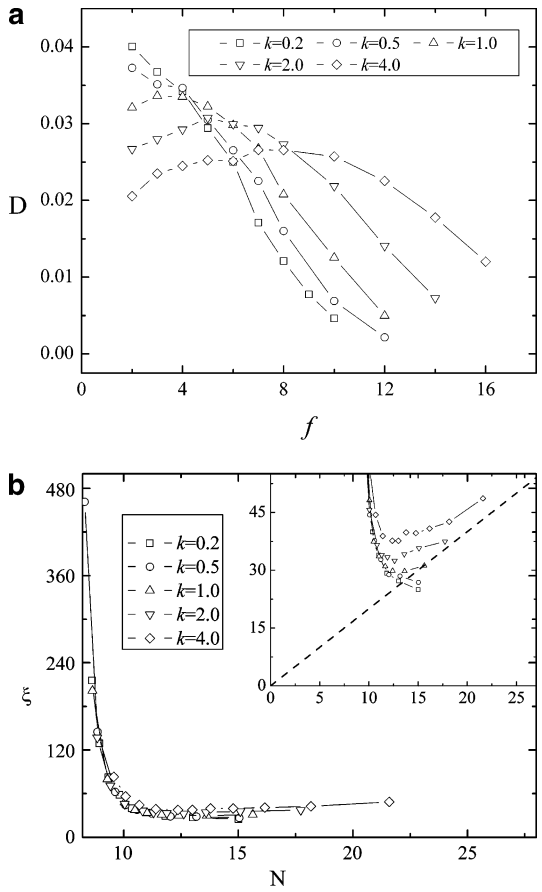

Figure 4. (a) The dependence of the diffusion coefficient of the knot of type 3_1 on the applied tension f for different values of the bending spring constant k. (b) Same data as in (a) plotted as the effective friction coefficient k_BT/D vs the knot length N. The dashed line is given by the equation $\xi = \xi_0 N$, where ξ_0 is the friction coefficient per one monomer (cf., **e**q 7). Inset: Same plot with the ξ scale blown up.

Both in Figure 3b and in Figure 4b, we find that for certain values of the bending stiffness and the force, the effective friction coefficient is somewhat *lower* than $\xi = \xi_0 N$ (the points below the dashed line). An effective friction coefficient that is higher than $\xi_0 N$ can be attributed to the contributions from the internal friction caused by monomer interactions within the knot, as those are neglected in eq 1. However finding the effective friction coefficient to be lower than $\xi_0 N$ is somewhat surprising. Consideration of chain fluctuations ignored in the sliding knot model may explain this observation. In particular, fluctuations of the knot size effectively speed up the diffusion. Indeed, if the instantaneous knot length N fluctuates significantly (cf., Figure 2) then the observed value of D will be the mean diffusion coefficient $\langle D \rangle = (k_BT/\xi_0)\langle 1/N \rangle$. If, for instance, the distribution of N is Gaussian (an approximation that is consistent with simulations), then $\langle D \rangle$ will be higher than an estimate obtained from eq 1 by using the mean knot length. The fairly small diffusion speedup found here is roughly consistent with an estimate of $\langle D \rangle$ that takes the knot size distribution into account. We note, however, that the deviations of real knot dynamics from the sliding knot model cannot be simply accounted for by allowing a distribution of the knot size N because both fluctuations of the knot itself and those of the unknotted segments of the chain affect the instantaneous value of N and also because knot fluctuations on a time scale comparable with that of the knot diffusion violate the assumptions of the sliding knot model.

Diffusion of Tight Knots. The knot diffusion coefficient depends on the properties of the chain (such as the bending stiffness k) and the tension f. However, in the tight knot limit (i.e., small N) D depends only on the knot size N rather than separately on the tension or the chain flexibility. That is, if we plot D (or ξ) vs $N(k,f)$ for various f and k, all these dependences will collapse onto a single curve. In particular, the curves $\xi(N)$ plotted in Figures 3b and 4b are practically identical for $N \leq 11$. Moreover, in this limit, unlike the large N case, more compact knots move more slowly. How can we rationalize these findings?

When the knot is tight, "internal friction" of the chain, rather than viscous friction due to the solvent, dominates its dynamics. The microscopic origin of such friction is the "bumpiness" of the energy landscape of the knot caused by the intrachain interactions.[23,24] The knot moves via activated barrier crossing from one local minimum to another. Indeed, stalling events where the knot is trapped in a local minimum configuration are readily observed in Figure 2 for the high-force case. The barriers encountered in this process depend on the magnitude of the tension in the chain. The higher the force f, the rougher the energy landscape and consequently the slower the diffusion.

Consider now the interactions within a tight knot. The forces associated with the bending potential V_{bend} in this limit become small as compared to the contribution from the repulsive potential $V_{nonbonded}$, which prevents the knot from becoming even tighter. A compact knot is a physical model of an "ideal" knot whose size can no longer be reduced[7,22] except that our compact knots are somewhat compressible since the repulsive interactions are continuous rather than hard-wall-type. The energy landscape in this limit is essentially determined by the repulsive interactions of the monomers within the knot, and it seems plausible that it would be determined only by the knot size.

Dependence of the Diffusion Coefficient on the Knot Type. We have computed the diffusion coefficient for several knot types (shown in Figure 1) and for different values of k and f. The results are shown in Figure 5, where the effective friction coefficient $\xi = k_BT/D$ is plotted as a function of the knot length N. The diffusion of the knots of type 3_1, 5_1, 5_2, and 7_1 is well described by the relationship $\xi \propto N$. The bulkier the knot, the slower it moves. Moreover, the ratio $\xi(N)/N$ for low forces is very close to the friction coefficient ξ_0 for a single monomer, again pointing to the local diffusion mechanism described by eq 1, which assumes a cooperative motion of N monomers in the knot region. The knot of type 4_1 seems to be an outlier except at high forces, possibly because of the knot fluctuations or a higher effective internal friction for this knot.

4. Discussion

Since our polymer model does not directly describe a DNA, to compare our results with the experimental findings of ref 18 we use reduced units of length and force. The characteristic length scale is set by the polymer's persistence length l_p and the characteristic force is set by $f_c = k_BT/l_p$. Assuming $l_p = 50$ nm, the forces used by Bao, Lee, and Quake are in the range $f \sim (1 - 25)f_c$. For such forces, they found the knot length to be $N \simeq 6l_p$(for the knot of type 3_1). To make a crude comparison with our results, consider the case $k = 1$ in Figure 4. At this value of the bending stiffness, the persistence length of our polymer is ~5 monomers, which gives $f_c \sim 0.2$ in the dimensionless units used in Figure 4a. We see that the experimental range of forces roughly corresponds to $f < 5$ in Figure 4a. The highest force in this range is close to the maximum of $D(f)$.

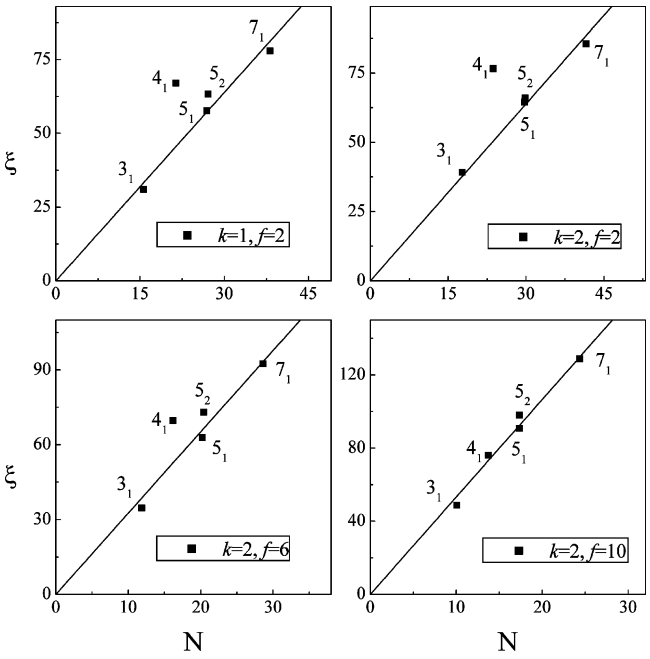

Figure 5. The effect of the knot type on its diffusion. The effective friction coefficient $\xi = k_BT/D$ plotted as a function of the knot length for different types of knots and for different values of the tension f and of the bending stiffness k. The straight lines shown are least-square fits with the knot type 4_1 excluded and are given by $\xi = aN$, where a = 2.13, 2.13, 3.26, and 5.33 for (k,f) = (1,2), (2,2), (2,6), and (2, 10), respectively.

To further validate this comparison we note that the knot length in this range of forces is $N \sim 3l_p$ for the lowest force used (cf., Figure 4b), which is comparable with the experimental knot length (measured in units of l_p).

These considerations suggest that the lack of tension dependence of the diffusion coefficient reported by Bao, Lee, and Quake[18]may be due to the fact that the experimental forces were close to the turnover regime, where—as we see from Figure 4a—the force dependence is weak.

The dependence of the effective friction coefficient ξ on the knot type observed in our simulations is very close to that reported in the experimental study (see Figure 3 in ref 18). Both the experimental curve $\xi(N)$ and the dependences shown in Figure 5 are close to linear. Moreover, the deviations of $\xi(N)$ from a straight line follow the same pattern. Our results are also consistent with the earlier simulation study by Vologodksii,[8] which includes electrostatic effects in DNA.

As seen from Figure 5, the linear dependence $\xi \propto N$ holds both at low forces (i.e., the elastic regime) and at high forces (tight knot regime), although the slopes are different. Therefore the linearity of this dependence alone cannot be used to distinguish between these two regimes and to establish whether or not DNA knots are close to ideal.

While the simple model considered here provides useful insights into the general problem of knot diffusion in tensioned polymers, a number of potentially important issues pertinent to DNA and proteins have been left out, particularly the effect of twisting, electrostatic effects, or of specific intrachain interactions on the knot dynamics. These effects may be particularly important in tight knots, where the strong constraints applied to the knot monomers may lead to high sensitivity of the knot dynamics to the details of the molecule's energy landscape. We plan to address these issues in our future studies.

Acknowledgment. We thank Ioan Andricioaei, Oscar Gonzalez, Ralf Metzler, Greg Rodin, and Peter Rossky for helpful discussions. This work was supported by the Robert A. Welch Foundation and by the National Science Foundation CAREER award to D.E.M. The CPU time was provided by the Texas Advanced Computer Center.

Appendix A: Distribution of the Knot Escape Time in the Free Diffusion Model

Suppose the knot's dynamics can be described as one-dimensional motion along the knot coordinate x. The knot starts in the middle of the chain at $x = 0$ and is monitored until it reaches one of the chain boundaries, $x(t) = \pm l/2$. We are interested in the probability distribution $p_{esc}(t)$ of the time t it takes the knot to escape the chain segment $(-l/2,l/2)$-between the boundaries. To find this, we first calculate the probability density $p(x,t)$ for finding the knot at x at time t provided that it disappears irreversibly upon reaching the boundaries. This is the solution of the one-dimensional diffusion equation

$$\frac{\partial p(x,t)}{\partial t} = D\frac{\partial^2}{\partial x^2}p(x,t) \tag{A1}$$

with the initial condition

$$p(x,0) = \delta(x) \tag{A2}$$

and absorbing boundary conditions at $x = \pm l/2$. The solution can be conveniently expressed as a series:

$$p(x,t) = \frac{1}{\sqrt{4\pi Dt}}\sum_{n=-\infty}^{\infty}(-1)^n \exp\left[-\frac{(x-nl)^2}{4Dt}\right] \tag{A3}$$

The probability distribution of the knot escape time can be expressed in terms of the knot survival probability:

$$S(t) = \int_{-l/2}^{l/2} p(x,t)\,\mathrm{d}x \tag{A4}$$

$$p_{esc}(t) = -\mathrm{d}S/\mathrm{d}t = -D\left[\frac{\partial p(x,t)}{\partial x}\bigg|_{x=l/2} - \frac{\partial p(x,t)}{\partial x}\bigg|_{x=-l/2}\right] \tag{A5}$$

Figure 6 gives an example of the distribution of the knot escape time determined from a simulation. The solid line is a fit that uses eqs A3−A5, with D being used as a fitting parameter. The free diffusion model fits our data very well.

Appendix B: Drag Force on the Knot Region in the Sliding Knot Model

Consider a continuous string with a knot tied in it. Here, we will assume that the knot slides along the string without changing its shape, as illustrated in Figure 7. The chain segments that are far away from the knot region are not moving; in particular, the chain ends are at rest. Assuming that the knot moves with a velocity v, we would like to calculate the total viscous drag force that acts on the chain. To do so, it is convenient to switch to a moving reference frame, in which the knot itself is at rest while each given point of the string is moving with a constant velocity along the same curve $(x(s),y(s),z(s))$, which defines the constant shape of the knot. Here $s = s_0 - vt$ is the position of the point measured along the string. The shape of the knot curve is such that $(x(s),y(s),z(s))$ = $(0,0,z)$ far away from the knot region. In other words, the

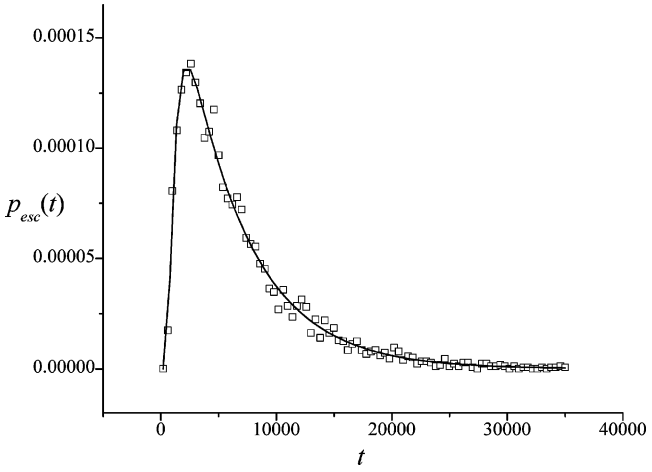

Figure 6. The probability distribution of the knot escape time fitted by using the free diffusion model (solid line). The values of the bending stiffness and the force in the simulation are $k = 2$, $f = 4$. The knot was placed in the middle of the chain and monitored until its distance from the middle attained the value $n(t) = \pm l/2$, where $l = 40$. The value of the diffusion coefficient obtained from this fit is $D = 0.0296$.

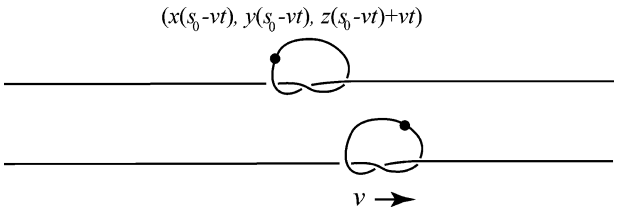

Figure 7. The sliding knot model. The time dependence of the position of a selected point on the string is shown.

string is a straight line aligned along the *z*-axis everywhere except in the vicinity of the knot.

The absolute value of the velocity of any given point of the string in the moving frame is equal to v while the velocity vector is given by

$$(\tilde{u}_x,\tilde{u}_y,\tilde{u}_z) = \frac{ds}{dt}\left(\frac{dx}{ds}, \frac{dy}{ds}, \frac{dz}{ds}\right) = -v\left(\frac{dx}{ds}, \frac{dy}{ds}, \frac{dz}{ds}\right) \quad \text{(B1)}$$

The velocity of the same point in the laboratory frame is

$$\mathbf{u} = (u_x,u_y,u_z) = (\tilde{u}_x,\tilde{u}_y,\tilde{u}_z) + (0,0,v) = -v\left(\frac{dx}{ds}, \frac{dy}{ds}, \frac{dz}{ds} - 1\right) \quad \text{(B2)}$$

The total viscous drag force on the chain is then given by

$$\mathbf{f}_{\text{drag}} = -\gamma_s \int_1^2 ds\mathbf{u}(s) \quad \text{(B3)}$$

where γ_s is the friction coefficient per unit length of the string and 1 and 2 denote the chain ends. Combining eqs B2 and B3 we find

$$\mathbf{f}_{\text{drag}} = -\gamma_s v(0,0, \int_1^2 (ds - dz)) = -\gamma_s v(0,0,\Delta z) \quad \text{(B4)}$$

where $\Delta z = \Delta z_{\text{unknotted}} - \Delta z_{\text{knotted}}$ is the difference between the end-to-end distance of the knotted and unknotted chains. The drag force is along the *z*-axis, and its value is proportional to the difference between the extension of the knotted and the unknotted chains.

For a discrete chain that consists of L monomers we can write $\gamma_s = \xi_0 L/\Delta z_{\text{unknotted}}$ (where ξ_0 is the friction coefficient per monomer) so that

$$f_{\text{drag}} = -\xi_0 N v \quad \text{(B5)}$$

where the effective number of monomers involved in the knot motion is given by

$$N = L\left(1 - \frac{\Delta z_{\text{knotted}}}{\Delta z_{\text{unknotted}}}\right) \quad \text{(B6)}$$

Supporting Information Available: Two animations of knot diffusion. This material is available free of charge via the Internet at http://pubs.acs.org.

References and Notes

(1) Kauffman, L. H. *Knots and Physics*; World Scientific: Singapore, New Jersey, London, Hong Kong, 2001.
(2) Frank-Kamenetskii, M. D. *Unraveling DNA*; Perseus Books: Reading, MA, 1997.
(3) Bates, A. D.; Maxwell, A. *DNA Topology*; Oxford University Press: Oxford, 2005.
(4) Taylor, W. R. *Nature* **2000**, *406*, 916−919.
(5) Saitta, A. M.; Soper, P. D.; Wasserman, E.; Klein, M. *Nature* **1999**, *399*, 46−48.
(6) Saitta, A. M.; Klein, M. *J. Phys. Chem.* **2001**, *28*, 6495−6499.
(7) Pieranski, P.; Przybyl, S.; Stasiak, A. *Eur. Phys. J. E* **2001**, *6*, 123−128.
(8) Vologodskii, A. *Biophys. J.* **2006**, *90*, 1594−1597.
(9) De Gennes, P. G. *Macromolecules* **1984**, *17*.
(10) Lobovkina, T.; Dommersnes, P.; Joanny, J.-F.; Bassereau, P.; Karlson, M.; Owar, O. *Proc. Natl. Acad. Sci U.S.A.* **2004**, *101*, 7949−7953.
(11) Grosberg, A. Y. *Phys. Rev. Lett.* **2000**, *85*, 003858.
(12) Metzler, R.; Reisner, W.; Riehn, R.; Austin, R.; Tegenfeldt, J. O.; Sokolov, I. M. *Europhys. Lett.* **2006**, *76*, 696−702.
(13) Ercolini, E.; Valle, F.; Adamcik, J.; Witz, G.; Metzler, R.; De Los Rios, P.; Roca, J.; Dietler, G. *Phys. Rev. Lett.* **2007**, *98*, 058102-1.
(14) Arsuaga, J.; Vazquez, M.; Trigueros, S.; Sumners, D. W.; Roca, J. *Proc. Natl. Acad. Sci. U.S.A.* **2002**, *99*, 5373−5377.
(15) Metzler, R.; Hanke, A.; Dommersnes, P. G.; Kantor, Y.; Kardar, M. *Phys. Rev. Lett.* **2002**, *88*, 188101-1.
(16) Kim, E.-G.; Klein, M. *Macromolecules* **2004**, *37*, 1674−1677.
(17) Arai, Y.; Yasuda, R.; Akashi, K.-i.; Harada, Y.; Miyata, H.; Kinosita, K.; Itoh, H. *Nature* **1999**, *399*, 446.
(18) Bao, X. R.; Lee, H. J.; Quake, S. R. *Phys. Rev. Lett.* **2003**, *91*, 265506-1.
(19) Arteca, G. A. *Phys. Chem. Chem. Phys.* **2004**, *6*, 3500−3507.
(20) De Gennes, P. G. *Scaling Concepts in Polymer Physics*; Cornell University Press: Ithaca, NY, 1979.
(21) Ben-Naim, E.; Daya, Z. A.; Vorobieff, P.; Ecke, R. E. *Phys. Rev. Lett.* **2001**, *86*, 1414.
(22) Gonzalez, O.; Maddocks, J. H. *Proc. Natl. Acad. Sci. U.S.A.* **1999**, *96*, 4769−4773.
(23) Kirmizialtin, S.; Makarov, D. E. *Phys. Rev. Lett.*, submitted.
(24) Persson, B. N. J. *Sliding Friction. Physical Principles and Applications*; Springer-Verlag: Berlin, Heidelberg, 1998.
(25) Harris, B. A.; Harvey, S. C. *J. Comput. Chem.* **1999**, *20*, 813−818.
(26) Vologodskii, A. V.; Lukashin, A. V.; Frank-Kamenetskii, M. D.; Anshelevich, V. V. *Sov. Phys. JETP* **1974**, *39*, 1059.